Measurement of Thermal Diffusivity Using Deformation Gradient and Phase in the Photothermal Displacement Technique

Pilsoo Jeon*, Kwangjai Lee
Department of Mechanical Engineering, Graduate School, Ajou University, Kyunggi-do, 442-749, Korea
Jaisuk Yoo, Youngmoo Park, Jonghwa Lee
Division of Mechanical and Industrial Engineering, Ajou University, Kyunggi-do, 442-749, Korea

As technology advances with development of new materials, it is important to measure the thermal diffusivity of material and to predict the heat transfer in the solid subject to thermal processes. The measurement of thermal properties can be done in a non-contact way using photothermal displacement spectroscopy. In this work, the thermal diffusivity was measured by analyzing the magnitude and phase of deformation gradient. We proposed a new data analysis method based on the real part of deformation gradient as the pump-probe offset value. As the result, compared with the literature value, the measured thermal diffusivities of materials showed about 3% error.

Key Words : Deformation Gradient, Photothermal Displacement, Phase, Thermal Diffusivity, Thermal Diffusion Length, Zero-Crossing Position

Nomenclature

a : Radius of pump beam (m)
f : Modulation frequency (1/sec)
k : Thermal conductivity (W/m·K)
L : Thickness of sample (m)
P_0 : Power of pump beam (W)
Q : Heat Source (W/m^3)
R : Reflectivity
r, z : Directions in cylindrical coordinate
T : Temperature (K)
u : Displacement vector (m)
α : Thermal diffusivity (m^2/sec)
α_{th} : Thermal expansion coefficient (1/K)
δ : Integral variable
λ : Absorption coefficient (1/m)
ν : Poisson's ratio
σ : Stress
ϕ : Displacement potential function
ψ : Love function

* Corresponding Author,
E-mail : stormdk94@orgio.net
TEL : +82-31-219-2350; **FAX** : +82-31-213-7108
Department of Mechanical Engineering, Graduate School, Ajou University, Kyunggi-do, 442-749, Korea.
(Manuscript **Received** April 2, 2003; **Revised** July 9, 2003)

1. Introduction

There has been the increase of interest in using photoacoustic and photothermal techniques to determine the structural, thermal, and optical properties of materials. Recently, the photothermal techniques based on photothermal radiometry, photothermal refraction, photothermal deflection, and photothermal displacement have been developed to measure the thermal diffusivity of solid or liquid (Chen and Mandelis, 1992 ; Cheng and Zhang, 1991 ; Salazar et al., 1991). In particular, the photothermal displacement method based on the modulated heating, developed in the early 1980s by Olmstead et al. and by Balageas et al. is generally used for thermal characterization or nondestructive testing of solid samples (Olmstead et al., 1983 ; Balageas et al., 1986).

The photothermal displacement uses basically two laser beams, one for heating the sample (pump) and the other (probe) to detect, through

the optical beam deflection effect, the produced thermoelastic deformation. The theoretical and experimental analyses of the photothermal displacement technique aiming at determining the thermal diffusivity have been performed by many authors (Ogawa et al., 1999 ; Jeon et al., 2002). In previous studies, thermal diffusivity was determined from a deformation curve, a phase curve, or a characteristic frequency. In order to determine the thermal diffusivity through a photothermal displacement, there are a few methods that minimize the error between the experimental and theoretical phase angle or deformation curve with a variable thermal diffusivity at the characteristic frequency. However, these methods have a relatively large error and need long time to analyze the experimental results because it is dependent on several optical and thermal properties. The phase curve and characteristic frequency methods require a complicated theory and a reference material, respectively. In this paper, we demonstrate that the thermal diffusivity can be very simply determined from the "minimum position" of phase curve and "zero-crossing position" of the real part of deformation gradient.

2. Theory and Principle

As shown in Fig. 1, the pump beam incident on the sample surface is absorbed by a sample of thickness L. The resulting deformation of the surface is observed by the deflection of a probe beam reflected from the surface of the sample at a pump-probe distance r. "Deflected" and "Undeflected"

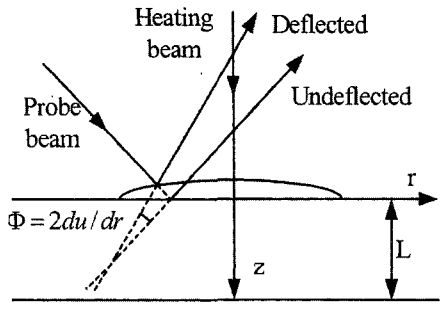

Fig. 1 The Principle of a measurement and theoretical model

refer to the paths of the probe beam after reflection with and without the deformation, respectively.

To obtain an expression for the photothermal deformation, we consider homogeneous and isotropic infinite plate of finite thickness (L) with stress-free boundaries, no thermal conduction to the surrounding gas, and irradiated by a sinusoidally modulated laser beam of power (P_0), incident on the sample normal to the sample surface (Jeon et al., 2002 ; Nowachi, 1986).

The temperature distribution within the sample is given by the solution of the following thermal conduction differential equation :

$$\nabla^2 T(r,z,t)+\frac{1}{k}Q(r,z,t)=\frac{1}{a}\frac{\partial T(r,z,t)}{\partial t}, \quad (1)$$

with boundary conditions

$$k\frac{\partial T}{\partial z}\Big|_{z=0,L}=0, \quad (2)$$

where $T(r, z, t)$ is the temperature in the sample, k is the thermal conductivity, a is the thermal diffusivity, and $Q(r, z, t)$ is the power deposited by the heating beam per unit volume.

The source term $Q(r, z, t)$ is described by a linear absorption of a Gaussian laser beam with $(1/e)$ radius that is modulated with frequency $f=\omega/2\pi$. We denote the total power of the incident Gaussian laser beam by P_0 and write for the source term,

$$Q(r,z,t)=\frac{\lambda P_0(1-R)}{4\pi a^2}e^{-r^2/a2-\lambda z}(1+\cos(\omega t)), \quad (3)$$

where R is the reflectivity, λ is the absorption coefficient, and a is the radius of pump beam. The heat source, $Q(r, z, t)$, consists of the time-independent and oscillating parts. But the time-independent part can be neglected because it does not contribute to the photothermal signal.

Due to the cylindrical symmetry of the problem, the differential equations describing the diffusion process can be solved by Hankel transform techniques. The solution for the temperature distribution is governed by an integral over single variable δ, representing the Hankel variable in the radial direction :

$$T(r,z,t)=-\frac{P_0(1-R)\lambda e^{i\omega t}}{8\pi k}\int_0^\infty \frac{\delta d\delta J_0(\delta r)\,e^{-\delta^2a^2/4}}{\lambda^2-\xi^2} \times\left[e^{-\lambda z}+\frac{\lambda\cosh(\xi z)}{\xi} \times\{\tanh(\xi z)-\coth(\xi L)+e^{-\lambda z}/\sinh(\xi L)\}\right] \quad (4)$$

where $J_0(\delta r)$ is the Bessel function of 0th order and $\xi=(\delta^2+i\omega/\alpha)^{1/2}$.

Assuming that the variation of the temperature field with time is small, the inertia terms in the thermoelastic equation may be neglected (Duhamel's assumption). Then, the thermoelastic equation with temperature $T(r, z, t)$ is given by

$$(1-2v)\nabla^2\vec{u}+\nabla(\nabla\cdot\vec{u})=2(1+v)\alpha_{th}\nabla T \quad (5)$$

with stress-free boundary conditions

$$\sigma_{rz}|_{z=0,L}=0,\ \sigma_{zz}|_{z=0,L}=0, \quad (6)$$

where v is the Poisson's ratio, $\vec{u}$ is the displacement vector, α_{th} is the thermal expansion coefficient, σ_{rz} and σ_{zz} are the two stress components, and T is the temperature rising, inside the sample, previously obtained in Eq. (4). Because of the geometry of the pump beam, the solution $u(r, z)$ can be expressed in cylindrical coordinates by introducing the displacement potential ϕ and the Love function ψ as follows:

$$\vec{u}=\nabla\phi\{2(1-v)\nabla^2\psi-\nabla(\nabla\cdot\psi)\}/(1-2v) \quad (7)$$

where ϕ and ψ are governed by the following differential equations

$$\nabla^2\phi=\frac{1+v}{1-v}\alpha_{th}T \quad (8)$$

$$\nabla^4\psi=0 \quad (9)$$

Note that, in order to express of the deflection angle, one needs only the normal component of the displacement u_z at $z=0$ so as to calculate the gradient in r as follows

$$\frac{\partial u_z}{\partial r}\Big|_{z=0}=\frac{(1+v)\alpha_{th}P\lambda^2}{2\pi kL}\int_0^\infty\frac{\delta^2 d\delta J_1(\delta r)\,e^{-\delta^2a^2/4}}{\lambda^2-\xi^2} \times\sum_{p=1}^{\infty}\frac{\eta_p^2H(\delta)[(-1)^p-\cosh(\xi L)]}{\xi(\delta^2+\eta_p^2)(\xi^2+\eta_p^2)\sinh(\xi L)}, \quad (10)$$

where $J_1(\delta r)$ is the Bessel function of first order and

$$H(\delta)=[\sinh^2(\delta L)+(-1)^p\delta L\sinh(\delta L)] \times[\delta^2L^2-\sinh^2(\delta L)].$$

For the known thickness of material and radius of the pump beam, the phase is determined by the integral term in Eq. (10), which is a complex number and a rather intricate integral term including thermal diffusivity, etc. In terms of the thermal diffusivity and the modulation frequency, the thermal diffusion length is given by $L_{th}=(\alpha/\pi f)^{1/2}$.

3. Experiment

The experimental arrangement is shown in Fig. 2. The pump beam is obtained by the acousto-optic modulation of a continuous-wave laser beam delivered by an Ar+ laser (wavelength: 488 nm), and typically, 0.7 W of energy was used to heat the sample. The beam power in front of sample decreases to 0.3 W approximately passing through the acousto-optic modulator, the lens, the mirrors, and the collimator. Considering the reflection of sample surface, the absorbed energy is estimated to be about 0.2 W. It was critically important for the pump beam spatial profile to be Gaussian. The typical pump beam spot size on the sample was approximately 55 μm in radius at the $1/e$ point. The probe beam is provided by a He-Ne laser (wavelength: 633nm), with a power of 10 mW and a beam diameter of 40 μm. The beam sizes on the sample surface were determined by the Knife-edge method. Both the pump and probe beams are expanded through collimators.

The pump beam is modulated at a frequency f to create a steady periodic thermoelastic deformation in the sample. The deflection of the probe

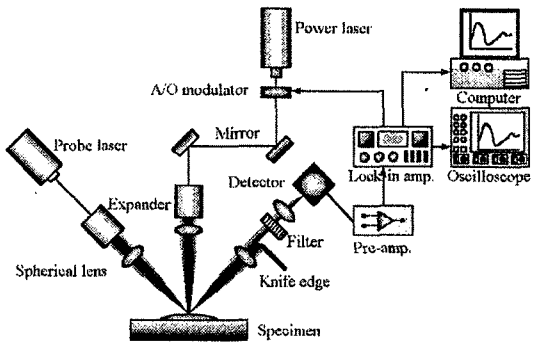

Fig. 2 Schematic diagram of experimental setup

Table 1 Optical and thermal properties of copper, iron, and zincc L, a, k, α_{th}, ν, R, and λ are the sample thickness, thermal diffusivity, thermal conductivity, thermal expansion coefficient, Poisson ratio, reflectivity, and optical absorption coefficient, respectively

	Copper (99.98%)	Iron (99.90%)	Zinc (99.80%)
L	0.82	1.04	0.78
$a\times10^5$	11.6	2.3	4.4
k	398	80.5	121
$\alpha_{th}\times10^6$	16.6	12	35
ν	0.35	0.28	0.35
R	0.640	0.610	0.747
$\lambda\times10^{-7}$	7.01	9.86	9.77

beam is measured by means of a Knife-edge and a photodiode (Bayazitoglu and Özisik, 1988). An interference filter is put in front of the photodiode to select only the probe beam wavelength. The amplitude and the phase of the signal are measured by a lock-in amplifier, which is synchronized at the modulation frequency.

The position of the probe beam is aligned with the centerline of the deformation. At the center of the deformation, the amplitude of the signal is minimized and the phase is oscillated. After aligning the probe beam and the pump beam positions, the measurement is carried out by traveling the probe beam along the centerline of the deformation. The probe beam is moved relative to the pump beam using an arrangement of mirrors and micropositioners. These micropositioners are controlled with an accuracy of ±0.5 μm. Experiments were carried out on samples of copper, iron, and zinc, which are polished using alumina paste. Optical and thermal properties of the samples are represented in Table 1.

4. Results and Discussion

Figure 3 shows the typical plot of temperature distribution at the surface. There is some difference according to the analysis condition such as sample thickness, thermal diffusivity, thermal conductivity, thermal expansion coefficient, reflectivity, and optical absorption coefficient, but the maximum difference of temperature is about 1~3K usually. Because the temperature increment is very small, the measured value in this study could be the thermal diffusivity of room temperature.

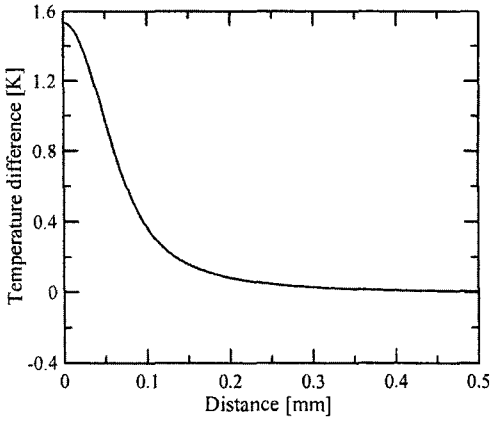

Fig. 3 Plot of temperature rise as a function of the distance r[mm] from the beam center. Parameters: using the thermal and optical properties of iron, $L=1$ mm, $a=55$ μm, $P_0=0.3$ W, $f=300$ Hz

Figure 4 shows the deformation gradient, phase and real part of deformation gradient at room temperature, the solid line represents the calculated result of Eq. (10). The theoretical predictions for the deformation the gradient and phase of the signal well correspond to the measured values. The deformation gradient and real part of deformation gradient curve were arbitrarily normalized. In Fig. 4(a), at pump-probe offset $r=0$, which is the center of the surface displacement, the deformation gradient of surface is zero, and therefore, the probe beam is not deflected and there is no signal at this point. Moreover, the signal becomes weaker and broader as r increases, as expected. The data for the opposite direction are not shown in Fig. 4, but the signal has a mirror image. The phase decreases up to a certain point, then starts to increase and approaches an asymptotic value. The phase has a position where the phase has a minimum value. The position p_{min} is defined as the "minimum position". The real part of deformation gradient is similar to the deformation gradient, but it has a

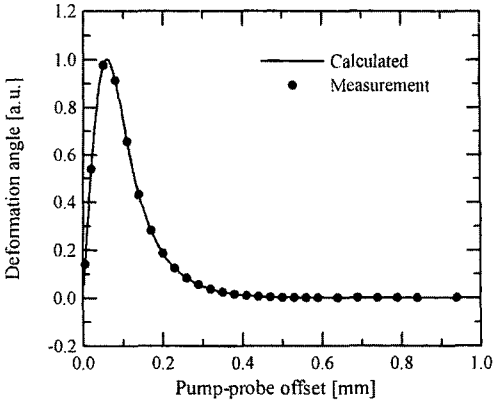

(a) Deformation gradient

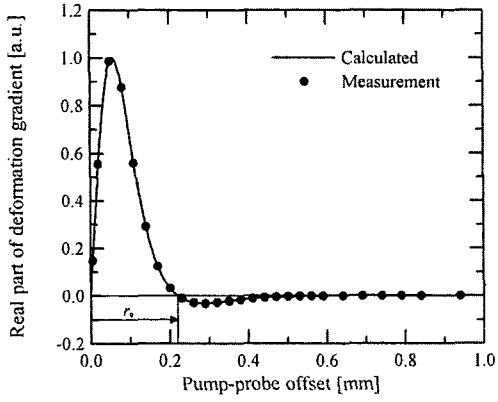

(b) Real part of deformation gradient

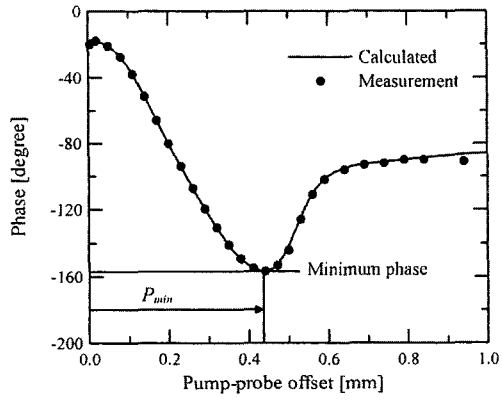

(c) Phase

Fig. 4 The deformation angle, phase angle, and real part of deformation gradient. Parameters : using the thermal and optical properties of iron, L=1 mm, a=55 μm, P_0=0.3 W, f=904 Hz

position where the real part of deformation gradient is zero. The position r_0 is defined as the "zero-crossing position". Both the minimum position and the zero-crossing position are functions of the thermal diffusion length, the sample thickness, and the radius of pump beam. Especially, the thermal diffusion length exerts the highest effect than other parameters.

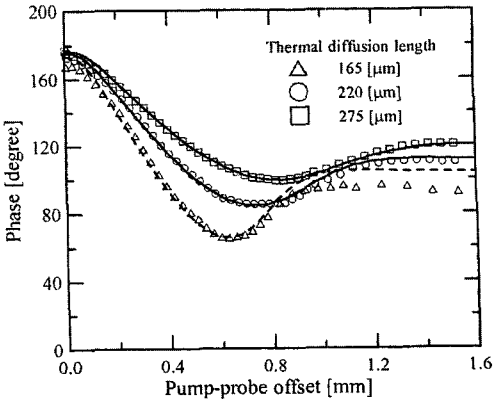

Fig. 5 Phase curve of copper for various thermal diffusion lengths

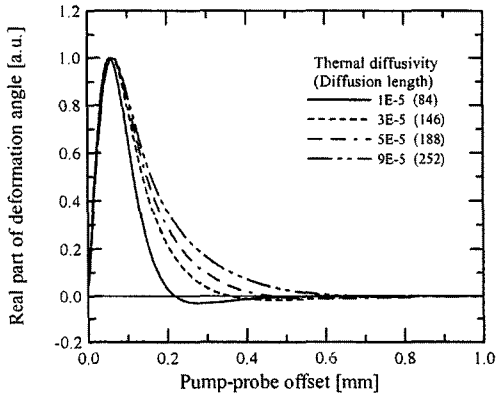

Fig. 6 Real part of deformation angle of various thermal diffusion lengths

Figures 5 and 6 show the phase and the real part of deformation gradient for various thermal diffusion lengths. The minimum position and the phase angle increase as the thermal diffusion length increases. Also, as the thermal diffusion length of experiment conditions such as the measuring material and the modulation frequency increases, the pump-probe offset distance where the real part of deformation gradient is zero should recede in the center of heating beam. This phenomenon occurs because the absorbed energy in the material of which thermal diffusivity is

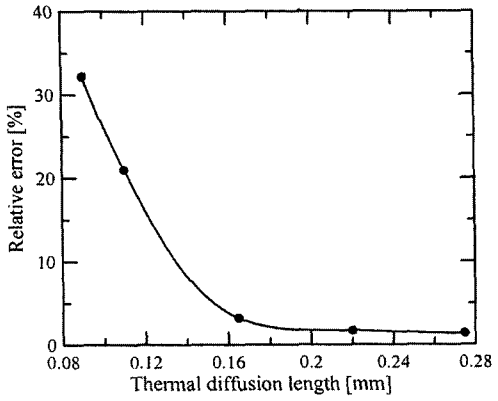

Fig. 7 The variation of thermal diffusivity for thermal diffusion length

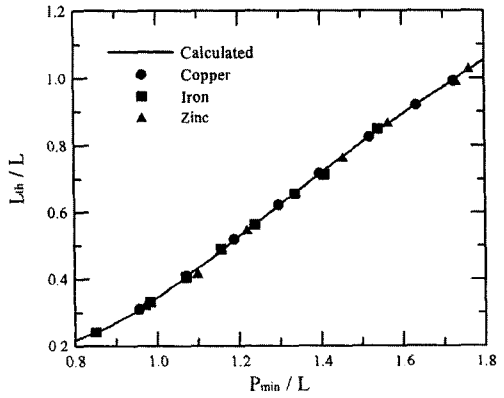

Fig. 8 Normalized minimum phase position versus normalized diffusion length

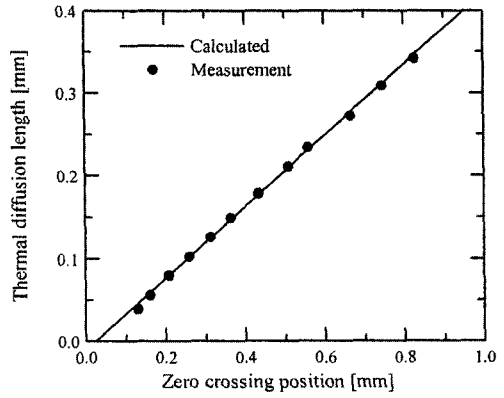

Fig. 9 Zero crossing position versus thermal diffusion length at radius of pump beam $a=55\ \mu m$

high, diffuses over the larger area than materials whose thermal diffusivity is relatively low. In addition, these results are caused by the fact that the absorbed energy in the materials per period reduces as the modulation frequency increases. So, the absorbed energy diffuses to a relatively small area.

In order to determine thermal diffusivity through photothermal displacement, there are a few methods that minimize the error between the experimental and theoretical phase angles or deformation curves with a variable thermal diffusivity at the characteristic frequency. But these methods have a relatively large error and need long time to analyze the experimental results. In this study, it is shown that the minimum position and zero-crossing position only depend on the thermal diffusion length and the pump beam radius. So considering this characteristic relation, as shown in Figs. 8 and 9, the simple equation is obtained from the fixed pump beam radius.

4.1 Phase curve

When the thermoelastic deformation in sample surface is generated by the pump beam, we can determine the thermal diffusivity from the relation phase curve and the pump probe offset value. The slope of the phase signal with respect to the relative position between the pump and the probe beam along the sample is quite sensitive to changes in the thermal diffusivity of the sample. The region where the measured and calculated phase curves agree well is from a quarter to three quarters of the minimum position. A thermal diffusivity is determined when the standard deviation between the measured and calculated phase curve changing the thermal diffusivity in Eq. (10) using a bi-section method, is minimized. Figure 7 shows the variation of relative errors, based on the measured value between measured thermal diffusivity and the literature value (Shackelford, 2000), against thermal diffusion length. In the case of a thermal diffusion length less than 1.5 times the pump beam diameter, the relative errors occurred about 20~30%. However, in the case of a thermal diffusion length greater than 1.5 times the pump beam diameter, the relative error is gradually reduced to 2~3%. And if the thermal diffusion length is greater than the sample thick-

ness, then the measured and calculated phase curves disagree because the assumption of insulation at the rear surface of the sample is not satisfied. Therefore, if the thermal diffusivity is to be determined from the phase curve, the range of the thermal diffusion length must be greater than the pump beam diameter and less than the sample thickness.

4.2 Minimum position

In Fig. 8, the thermal diffusion length normalized to the thickness of sample, L_{th}/L, is plotted versus the minimum position normalized to the thickness of sample, p_{min}/L. When the radius of the pump beam is 55 μm and the sample thickness is greater than 0.5 mm, the best fitting relation between normalized thermal diffusion length and normalized minimum position is given by the 5th order polynomial expression as follows

$$\frac{L_{th}}{L}=\sum_{n=0}^{5}A_n\left(\frac{p_{min}}{L}\right)^n. \tag{11}$$

where $A_n(n=0, 1, \cdots, 5)$ are 2.93, -10.29, 13.77, -8.11, 2.29, and -0.25, respectively. From the definition of thermal diffusion length, the thermal diffusivity is determined easily and simply. For the known sample thickness and the radius of the pump beam, therefore, thermal diffusivity is determined by the measurement of the minimum position.

The minimum position of the phase is determined by using a multi-parameter fitting of the experimental data, and then the thermal diffusivity is obtained from Eq. (11). Since the phase of the signal is not stable where $r<a$ and r is also near the asymptotic value, these data were not used for the fitting procedure. In experiments, when $L_{th}/L>0.9$, low modulation frequency corresponds to large thermal diffusion length and small variation of phase difference for r. Therefore, it is difficult to determine the minimum position. For $L_{th}/L<0.9$, several different modulation frequencies were used and the thermal diffusivities corresponding to the different modulation frequencies were obtained. It was found that the maximum difference is within 3% of the literature value. In the case of copper with 0.82 mm thickness, the typical range of frequency is from 80 Hz to 568 Hz. Figure 8 shows the experimental results for copper, iron, and zinc, plotted versus the theoretical curve [Eq. (11)]. Regardless of materials, the quantitative agreement between the theoretical curve and experimental result is excellent.

4.3 Zero-crossing position

Salazar et al. noted that for monolithic materials the first non-central zero of the variation of the in-phase or "real" part of the tangential component of the beam deflection varies linearly with inverse root frequency on the photothermal deflection method (mirage method). In this paper, this feature on mirage method applies to the photothermal displacement method (Salazar et al., 1989).

It is known that the zero-crossing position depends only on the thermal diffusivity, the pump beam radius and the modulation frequency. Considering this relation, as shown in Fig. 9, the simple relation equation is obtained at the fixed pump beam radius. There is a linear relation between the zero-crossing position and thermal diffusion length $(\alpha/\pi f)^{1/2}$ that is determined by the thermal diffusivity and the modulation frequency like Fig. 9. Therefore, the zero-crossing position is found from this relation and the thermal diffusivity can be easily obtained from it. However this technique cannot be applied to the materials or experimental conditions whose L_{th}/L is higher than 0.4, due to the disappearance of the zero. And when $L_{th}/L<0.2$, the best fitting relation between r0 and thermal diffusion length is in the form of the linear expression in Eq. (12).

$$L_{th}=C_1r_0+C_2 \tag{12}$$

Like Eq. (13), thermal diffusivity is determined by a simple equation from the definition of thermal diffusion length and Eq. (12)

$$\alpha=\pi f[C_1r_0+C_2]^2 \tag{13}$$

where the pump beam radius is 55 μm, C_1 and C_2 are 0.431 and -9.912×10^{-3}, respectively.

It is a merit that the thermal diffusivity can be determined very easily at a fixed pump beam

Table 2 Comparison of the measured thermal diffusivity and literature value (Shackelford, 2000). α_1, α_p, α_m, and α_2 are literature value, measured thermal diffusivity using phase curve, measured thermal diffusivity using minimum position, and measured thermal diffusivity using zero-crossing position, respectively

	Thermal diffusivity ($\times 10^5$[m^2/s])			
	α_1	α_p	α_m	α_2
Copper	11.6	11.54	11.5	11.29
Iron	2.3	2.33	2.29	2.36
Zinc	4.4	4.43	4.39	4.26

radius using the relation presented in this study between the thermal diffusion length and zero-crossing position. It was found that the maximum difference is about 3% of the literature value when $L_{th}/L<0.2$. Regardless of the material and the sample thickness, the quantitative agreement between the theoretical curve and experimental result is excellent as shown in Fig. 9.

These methods of converting of the measured minimum position of the phase and the zero-crossing position of the real part of deformation gradient to the thermal diffusivity by a simple correlation is very convenient compared to other methods. An interesting feature of the method is a direct measurement of the thermal diffusion length. In Table 2, the results obtained by our methods are compared with literature values (Shackelford, 2000).

5. Conclusions

In conclusion, we improved the method of analysis for the determination of thermal diffusivity using the photothermal displacement method. To measure the thermal diffusivity easily and precisely, we consider the "minimum position" where the phase has a minimum value and the "zero-crossing position" where the real part of deformation gradient is zero. Through the relation between the thermal diffusion length and these value, the following conclusions are obtained:

(1) As the thermal diffusion length, r_0 becomes more distant from the center of pump beam, the minimum point of phase angle becomes more distant as well.

(2) The relation between the thermal diffusion length normalized to the sample thickness (L_{th}/L) and the minimum position normalized to the sample thickness (p_{min}/L) is the same for all materials. And the zero-crossing position (r_0) is linear to the thermal diffusion length. Applying these methods, it is very simple and easy to determine the thermal diffusivity with accuracy.

(3) The experimental data obtained by applying these methods for different samples were in good agreement with the literature values.

(4) The value of the thermal diffusivity is derived from the minimum position and zero-crossing position of the photothermal signal. Therefore, the analysis is independent of the laser power and many properties of the sample such as its absorption coefficient, reflectivity, Poisson ratio, thermal expansion coefficient, etc.

Acknowledgements

This work was supported by NRL (National Research Laboratory) Program of the Ministry of Science and Technology, Korea.

References

Balageas, D. L., Krapez, J. C. and Cielo, P., 1986, "Pulsed photothermal modeling of layered materials," *J. Appl. Phys.*, Vol. 59, No. 2, pp. 348~357.

Bayazitoglu, Y. and Özisik, M., 1988, *Elements of Heat Transfer*, McGraw Hill, New York.

Chen, Z. and Mandelis, A., 1992, "Thermal diffusivity measurements of ultrahigh thermal conductors with use of scanning photothermal rate-window spectrometry: Chemical-vapor-deposition diamonds," *Phys. Rev.* B, Vol. 46, pp. 13526~13538.

Cheng, J. C. and Zhang, S. Y., 1991, "Three-dimensional theory to study photothermal phenomena of semiconductors. I. Modulated optical reflectance," *J. Appl. Phys.*, Vol. 70, No. 11, pp. 6999~7006.

Jeon, P. S., Lee, K. J., Yoo, J. S., Park, Y. M. and Lee, J. H., 2002, "Measurement of thermal diffusivity using deformation angle based on the photothermal displacement method," *Transactions of the KSME*, B, Vol. 26, No. 2, pp. 302~309.

Nowacki, W., 1986, *Thermoelasticity*, 2nd ed, Pergamon Press.

Ogawa., E. T., Hu, C. and Ho, R. S., 1999, "Thermal diffusivity measurement of polymer thin films using the photothermal displacement technique. I. Free-standing film case," *J. Appl. Phys.*, Vol. 86, No. 11, pp. 6018~6027.

Olmstead, M. A., Amer, N. M. and Kohn, S., 1983, "Photothermal Displacement Spectroscopy : An Optical Probe for Solids and Surfaces," *Appl. Phys.* A, Vol. 32, pp. 141~154.

Salazar, A., Sanchez-Lavega, A. and Fernandez, J., 1989, "Theory of thermal diffusivity determination by the "mirage" technique in solids", *J. Appl. Phys.*, Vol. 65, pp. 4150~4156.

Salazar, A., Sanchez-Lavega, A. and Fernandez, J., 1991, "Thermal diffusivity measurements in solids by the mirage technique : experimental results," *J. Appl. Phys.*, Vol. 69, No. 3, pp. 1216~1223.

Shackelford, J. F., 2000, *CRC Material Science and Engineering Handbook*, 3rd ed, CRC Press.